Journal of Colloid and Interface Science **216,** 134–142 (1999)
Article ID jcis.1999.6260, available online at http://www.idealibrary.com on IDEAL®

3D Monolayers of 1,4-Benzenedimethanethiol on Au and Ag Clusters: Distinct Difference in Adsorption Geometry with the Corresponding 2D Monolayers

M. Venkataramanan,* Shuguang Ma,† and T. Pradeep*,[1]

*Department of Chemistry and Regional Sophisticated Instrumentation Centre, Indian Institute of Technology, Madras 600 036, India; and †Department of Chemistry, Purdue University, West Lafayette, Indiana 47907

E-mail: pradeep@iitm.ernet.in.

Received January 21, 1999; accepted March 30, 1999

Au and Ag clusters of 3-nm mean diameter were prepared with 1,4-benzenedimethanethiol (BDMT) as the capping molecule. In both the monolayer-capped clusters, BDMT adsorbs in the dithiolate form in contrast to in the 2D monolayers, where the dithiolate form exists only in the case of Ag. As a result, the molecule lies flat on the cluster surface in both Au and Ag, whereas the molecular plane is perpendicular to the surface in the 2D monolayer of Au. This difference in adsorbate structure is attributed to the evolution in the cluster surface as adsorption occurs. Transmission electron microscopy and X-ray powder diffraction suggest that no superlattice of the clusters exists. Mass spectrometry suggests the presence of the phase transfer reagent at the surface. X-ray photoelectron spectroscopy confirms the chemical similarity of the two surfaces and suggests that the thiolate at the surface is susceptible to X-ray beam induced damage.

Key Words: **monolayer-protected clusters; self-assembled monolayers; Fourier transform-infrared spectroscopy; transmission electron microscopy.**

INTRODUCTION

Monolayer protected clusters (MPCs) (1) belong to an important family of nanophase materials that are being investigated currently due to their diverse physico-chemical properties and potential applications (2). The principal interaction stabilizing the clusters is the specificity of the molecule–metal bonding. Molecules with a number of head and tail groups can be made to bind different surfaces (3), and it is possible to synthesize clusters with diverse properties. A range of cluster sizes can also be prepared by appropriate manipulation of the kinetic parameters (4). Apart from the properties of the metal core, the molecular chemistry of monolayers has also attracted attention (5). The diversity of the chemistry of self-assembled monolayers (SAMs) (6) grown on planar surfaces (2D SAMs) can be directly adapted to monolayers on cluster surfaces (3D SAMs) (7). The advantage of high molecular coverage owing to the large surface area has made it possible to investigate monolayers by a host of analytical techniques, which are impossible to use with 2D monolayers (7a). Thus there have been structural and spectroscopic studies. Electrical transport properties (8), phase transitions of the alkyl chains (9), reactivity of the terminal groups (10), and exchange behavior (11) of the adsorbates have all been studied. Most of these investigations have been centered around the Au–alkanethiol system, mostly because of the wealth of knowledge of the corresponding 2D SAMs (12, 13). However, relatively little knowledge exists on the corresponding Ag system (7h, 14), although there are studies on some of the important aspects such as structure, cluster size, and self-organization (7h).

The most important difference between the 2D and 3D SAMs is that the surface on which adsorption occurs in the latter is three dimensional—as the name itself indicates. This would make the molecules at the surface diverging as they move away from the metal. Due to this, there is a definite possibility of the interpenetration of the monolayers of the adjacent clusters in the solid state. Such an interaction has indeed been observed, and it has been manifested in the phase transition of 3D SAMs (7a, 9). Interdigitation of molecules within 3D SAMs leading to bilayers has also been observed (15). This in fact is one of the deviations from the corresponding 2D SAMs, which are well ordered with almost crystalline-like assembly of the molecules.

In this paper, we wish to explore other differences between the 2D and 3D SAMs. As there is little difference between the adsorption of monofunctional molecules on planar and curved surfaces, we chose to investigate the differences in the adsorption of bifunctional molecules. In a recent investigation of the adsorption of 1,4-benzenedimethanethiol (BDMT) on planar surfaces we showed that whereas it adsorbs with one thiol group in the case of Au, both the thiol groups are bonded with the surface in the case of Ag (16). This difference in binding leads to completely different adsorbate geometries for both these surfaces. In the case of Au, the molecule stands perpen-

[1] To whom correspondence should be addressed.

0021-9797/99 $30.00

dicular to the surface whereas it is parallel to the surface on Ag. This is manifested in the surface-enhanced Raman spectra of both these systems, which show differences in enhancement for certain modes in these two geometries according to the selection rules. As a result of the geometry, the monolayer on Au shows temperature-dependent changes in orientation (16). The molecule falls on the surface and then desorbs upon heating. There is no such change for the Ag monolayer. The adsorption geometry also affects reactivity. Whereas the Au surface upon exposure to a thiol forms a bilayer, the Ag surface is unaffected.

In the study outlined below, we prepared BDMT-capped clusters of Au and Ag. The clusters were subjected to detailed investigations by transmission electron microscopy (TEM), X-ray diffraction (XRD), temperature-dependent infrared spectroscopy, X-ray photoelectron spectroscopy, and mass spectrometry. It is shown that the adsorption geometry of the molecule on both the surfaces is the same. Both the thiol groups are involved in bonding, in the thiolate form. In both cases, the benzene ring lies flat on the surface, resulting in poor intensity for the aromatic C—H stretching modes. Temperature-dependent changes in the infrared spectra are minimal. Although it is possible for the molecule to bind to two adjacent clusters, such a binding is not observed and no superlattice of the clusters is formed this way. The two-phase synthesis leads to the adsorption of the phase transfer reagent on the surface, which is detected in mass spectrometry. It is suggested that the availability of proper adsorption sites at the appropriate distance makes it possible for both the thiol groups to anchor on the surface. This appears to be due to the curvature of the surface. The kinetics of adsorption and cluster growth also influences the adsorption geometry.

EXPERIMENTAL

The cluster compounds were synthesized using a procedure from the literature (3a). Briefly, 10 ml 0.0288 M aqueous hydrogen tetrachloroaurate (Merck, 99%; $AgNO_3$, 99.99% in the case of silver clusters) was extracted into toluene (23.8 ml) using tetraoctylammonium bromide (Merck, 98%) as the phase transfer reagent upon vigorous stirring. The resulting organic phase was then mixed with an equimolar amount of 1,4-benzenedimethanethiol (Aldrich, 99%) and was subsequently reduced using an approximately tenfold molar excess (9 ml) of aqueous sodium borohydride (Aldrich, 99%), which was added drop-wise. The addition was completed in about 1 h. The solution was stirred overnight at room temperature. The black precipitate obtained was washed well with toluene to remove the excess thiol. The samples were filtered and dried. They were found to be insoluble in organic solvents, and therefore, no optical absorption or nuclear magnetic resonance spectra were measured.

Transmission electron micrographs were taken with a 200 keV JEOL JEM-2000EX microscope at Purdue University. A drop of the dilute toluene dispersion of the cluster was put on a holey carbon grid and was allowed to dry in air.

X-ray diffraction patterns were measured with Cu$K\alpha$ radiation. The samples were spread on antireflection glass slides to give uniform films. The films were wetted with acetone for adhesion and were blown dry before measurement. All samples were similarly prepared.

The infrared spectra were collected in the transmission mode with a Bruker IFS 66v FT-IR spectrometer. A KBr pellet was prepared by mixing approximately 1 mg of the sample with 1 g potassium bromide. The spectra acquired were averages of 200 scans which were background subtracted automatically. Temperature-dependent infrared spectra were measured with a variable temperature accessory developed in the laboratory.

X-ray photoelectron spectra were recorded with a VG ESCALAB Mk II spectrometer using unmonocromatized Al$K\alpha$ radiation as the excitation source. The binding energies are referenced to Au $4f_{7/2}$ peak at 84.0 eV. The monolayers showed no effect of charging during the measurements. No desorption was noticed during the measurements. The electron flux was kept at 70 mW to keep the beam-induced damage low. Each spectrum was an average of 20 scans of 2 min duration. The spectra were acquired in the constant analyzer energy mode. A pass energy of 50 V was used for the C, O, Au, and Ag regions, and 100 V measured for the S2p region.

Mass spectra were recorded with a TSQ700 triple quadrupole spectrometer. Samples were introduced as powders, coated on a heating filament, and heated up to 1473 K in a programmed fashion. Spectra acquired around the maximum in the total ion current were averaged and are reported as the mass spectra of the samples. Collision-induced dissociation spectra of several ions were done to make peak assignments. The ion of interest was mass selected ($\Delta m = 1$ amu) by the first quadrupole and was collided with Ar (0.4 mTorr) in the second quadrupole at 10 eV translational energy. The collision induced dissociation spectra were measured with the third quadrupole.

RESULTS AND DISCUSSION

Transmission Electron Microscopy and X-Ray Powder Diffraction

Figure 1 shows the TEM images of the gold and silver clusters capped with BDMT. The average cluster size is about 4 nm although a range of sizes from 2 to 6 nm are observed. No superlattice formation is evident, which would have been the case had each of the functional groups of the BDMT molecule been bound to two separate clusters in a regular fashion. Geometrically this is not possible, as the size of the clusters is much larger than the dimensions of BDMT, and therefore, not all the molecules can be involved in intercluster bonding. However, it is possible for a small fraction of the adsorbates to

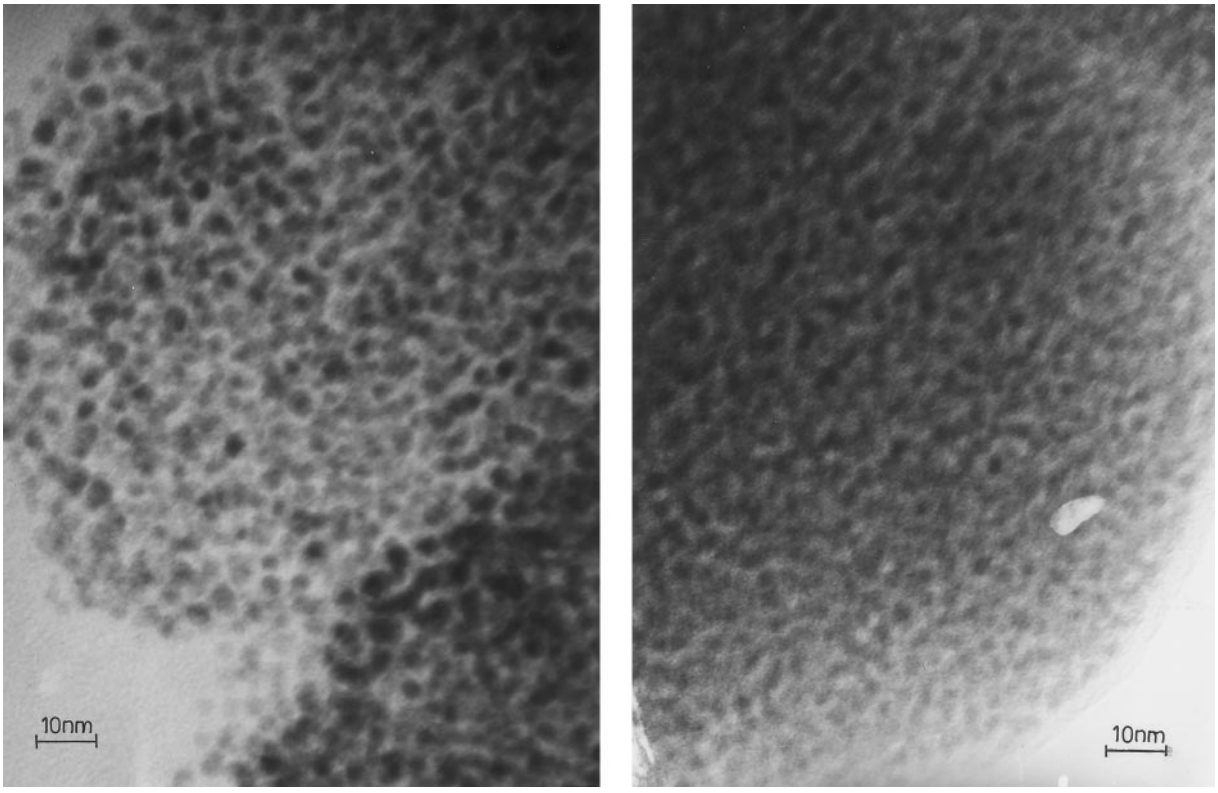

FIG. 1. The left and right figures correspond to transmission electron micrographs of Au and Ag clusters capped with BDMT, respectively.

do so, and this should be the reason for the agglomeration of the particles, making them insoluble in organic solvents.

X-ray powder diffraction patterns of the samples show bulk reflections. No small angle reflection is seen in the spectra. An analysis of the peak-width using the Schrerer formula (17) gives a cluster size of 4 nm for the Au cluster, in agreement with the TEM data.

Fourier Transform-Infrared Spectroscopy

Figure 2 shows the FT-IR spectra of (a) the BDMT solid and BDMT capped (b) Au and (c) Ag clusters. The inset shows the corresponding C—H stretching regions. The assignments of the peaks are given in Table 1. The S—H stretching of the BDMT solid occurs at 2552 cm^{-1}, which is completely absent in the Au and Ag clusters, indicating dissociative chemisorption on the surfaces. This shows that the nature of binding is similar in both clusters. There are certain differences in the relative intensities of the bands upon adsorption. The methylene symmetric stretch at 2856 cm^{-1} increases in intensity. Part of this enhancement we attribute to the presence of small quantities of the phase transfer reagent that is manifested in the mass spectrum of the sample (see below).

Another characteristic difference observed is the downshift of the aromatic stretching frequencies upon adsorption. The shift to lower frequencies is considerably larger in the silver cluster. It may be noted that a shift of about 5–10 cm^{-1} for these bands was observed in the case of the 2D monolayers of Au and Ag (16). The shift of the aromatic stretching frequency is attributed to the surface–ring π interaction, which is greater in the case of silver, suggesting a more parallel arrangement of the phenyl ring to the surface. This kind of surface geometry is also suggested by the lower intensity of these peaks compared to Au. The intensity is understandable from the infrared selection rules (18), which say that a change in the dipole moment perpendicular to the surface is necessary for a mode to get excited. The aromatic C—H mode is parallel to the surface and is expected to be weak when the ring is parallel to the surface. This suggestion of adsorption geometry is prone to error since the clusters are randomly oriented and the IR radiation is not polarized. It is to be noted that the same reduction in intensity is observed on all other bands except the aliphatic C—H stretching modes in the case of Ag, which again supports the suggestion. In order to compare the intensities, the spectral intensities are not manipulated. Since the intensities are not corrected for sample thickness and concentration, absolute intensities are not comparable and our comparison is only based on relative intensities in a given spectrum.

The ring C—C stretching vibrations occurring at 1512 cm^{-1} for the solid shift slightly to lower frequency upon adsorption to Au and Ag clusters. The bands occurring at 1418 and 1430

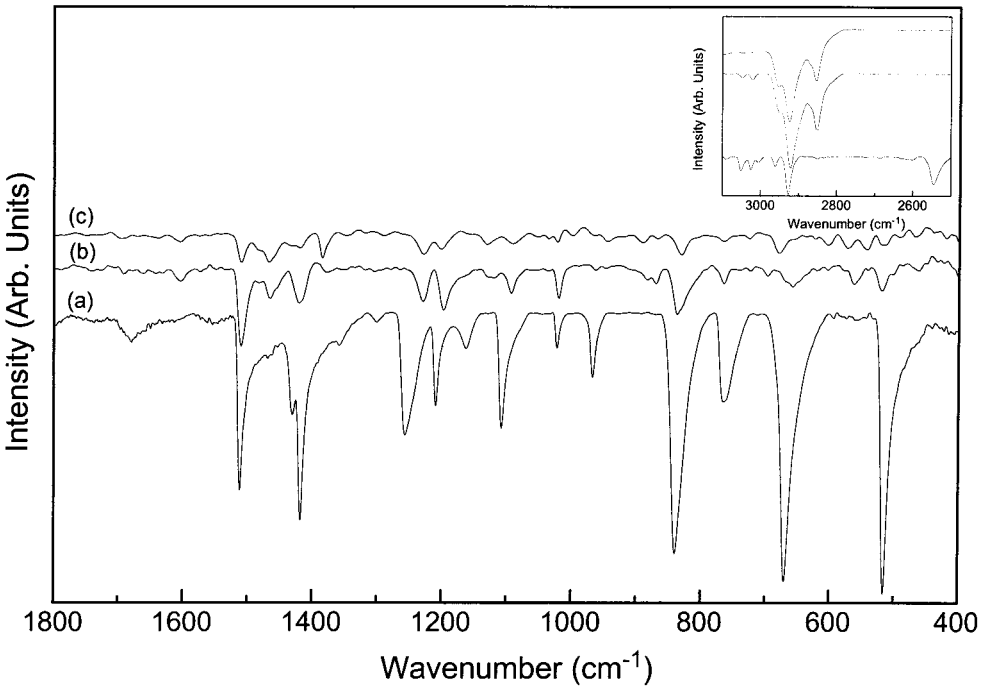

FIG. 2. The FT-IR spectra of (a) the BDMT solid and BDMT capped on (b) Au and (c) Ag clusters. The corresponding C—H regions are shown in the inset. Intensities are plotted in the same scale but have not been corrected for sample thickness or concentration.

(shoulder) for the solid correspond to the methylene scissoring modes (19), which do not get shifted upon adsorption. The shifts in the wagging modes are greater upon adsorption. The peaks, which appear at 1255 and 1209 cm^{-1} for the solid, are downshifted to 1228 and 1195 cm^{-1}, respectively, upon adsorption. These observations indicate that the chemical environment around methylene groups changes drastically upon adsorption. One important aspect to note is that in the case of both Au and Ag, the peak shape and the shift of both these bands are similar, and this is significantly different from the corresponding 2D SAMs.

The C—S stretching frequency for the solid appears at 670 cm^{-1}. This band red-shifts to 659 cm^{-1} upon adsorption; the shift is comparable to that observed in the Raman spectra (16). The intensity of this band is considerably reduced upon adsorption, in contrast to the Raman spectra (16). Again it is attributed to the adsorption geometry in which the C—S bond is predominantly parallel to the surface. Whereas the C—S stretching band is relatively well defined in the case of Au, it is broader for Ag, presumably due to the presence of different adsorption sites.

The peak appearing around 763 cm^{-1} is a result of ring breathing motion (19). This motion does not change much upon adsorption to gold and silver clusters. The out-of-plane ring vibrations give rise to a peak around 835 cm^{-1}, which also does not change upon adsorption.

In addition to these features there are also weak features, for example, at 1385 and 1350 cm^{-1} for the Ag–BDMT cluster, which are due to the phase transfer reagent (PTR) used in the cluster synthesis. The mass spectrum for the cluster also gives evidence for the presence of PTR (see below).

As discussed above, the shifts of certain peaks and the absence of S—H stretching frequency for the monolayers clearly indicate the adsorption of BDMT molecules to the Au and Ag cluster surfaces. The complete absence of S—H stretching in the case of gold clusters is in contrast with the result observed for the same monolayer on flat Au surfaces (2D SAMs). In the latter case, the benzene ring lies perpendicular to the surface, which results in one S—H group poking at the surface whereas the other is bound to the surface in the thiolate form. The free thiol proton on the surface of the 2D SAM undergoes exchange reactions on exposure to other thiols in solution phase reactions. This difference in adsorption geometry between 2D and 3D SAMs is presumably due to differences in the two surfaces. In the case of 2D SAMs, the surface is already available and no additional surface binding site is created as the adsorption occurs, so all the incoming thiol molecules are adsorbed on Au(111) planes to form a densely packed arrangement. But, in 3D SAMs, the cluster growth occurs during the thiol addition and capping arrests the cluster growth. Therefore, it may be possible for the incoming thiol molecule to find two adsorption sites at a distance matching the separation between two sulfur atoms in the BDMT molecule as it approaches the cluster surface. It is also likely that the adsorption initially occurs at one site and as the cluster growth occurs, the other thiol group also gets bound to the new site

TABLE 1
Comparisons of IR Vibrational Frequencies of BDMT on Au and Ag Clusters with those of BDMT in the Solid State

BDMT solid[a]	BDMT on Au cluster[a]	BDMT on Ag cluster[a]	Assignment
515	516	523	
	557	560	
669	659	676	ν C—S
763	764	764	Ring breathing mode
835	833	831	Out-of-plane ring vibrations
962	961(vw)	961(vw)	
1020	1018	1018	
1106	1090	1091	In-plane ring modes
1209	1195	1198	do
1255	1228	1228	CH_2 wagging
1418	1417	1417	CH_2 scissoring
1430(sh)	1462	1466	
1512	1509	1509	Ring C—C deformation
	1602	1602	
2552	—	—	ν S—H
2856	2850	2853	ν C—H symmetric
2930	2920	2922	ν C—H antisymmetric
2965	2951	2952	ν C—H (of methyl)
3028	3021	3018	ν C—H (ring)
3057	3048	3045	ν C—H (ring)

Note. vw, very weak; sh, shoulder.
[a] In cm^{-1}.

created. Thus it is suggested that the kinetics of adsorption is comparable to that of cluster growth, which is likely since both are chemical reactions. In any case, the difference in the nature of binding due to difference in shape is interesting. We will come back to this in a later section.

Variable Temperature Infrared Spectroscopy

The variable-temperature IR spectra of BDMT on the Au cluster are shown in Fig. 3. In the case of BDMT 2D SAMs on Au, a variable temperature surface-enhanced Raman spectroscopic (SERS) study indicates that the molecule falls down on the surface upon increase in the temperature (16). In the case of 3D SAMs, as the temperature is increased, the CH_2 wagging modes appearing at 1228 and 1198 cm^{-1} undergo reversal in intensity (Fig. 3). All peaks undergo decrease in intensity upon increase in temperature due to desorption of monolayers from the cluster surface. Also, the ring vibration occurring at 1507 cm^{-1} splits into two peaks around 473 K. In order to compare the intensities, all of the spectra collected under identical conditions are plotted in the same intensity scale. All of the above observations indicate that structural changes are happening to the monolayers on increase in temperature, particularly with respect to the CH_2 moieties.

The effects of structural changes are not particularly noticeable on the C—H stretching modes. We find neither a systematic shift nor a change in the intensity pattern. A gradual reduction in intensity with temperature is noticeable on both the bands as a result of desorption. The ring deformation mode also does not show a systematic shift. All of these together suggest that there is no significant difference in the ring–cluster interaction with increase in temperature. Thus the kinds of structural changes are limited to increases in orientational freedom of the molecule at the cluster surface, presumably around the methylenes.

In the case of BDMT on silver clusters (Fig. 4), there is no change in peak positions or intensity reversal (particularly for

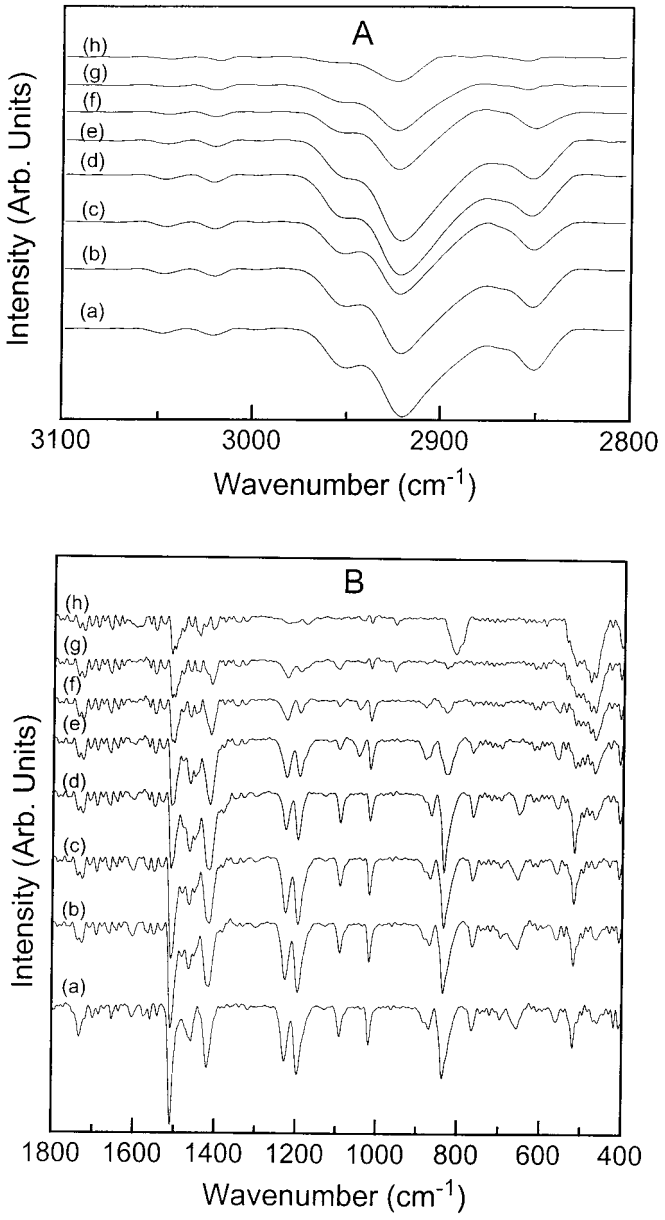

FIG. 3. Variable-temperature FT-IR spectra of BDMT-capped gold clusters. The temperatures are (a) 298, (b) 323, (c) 348, (d) 373, (e) 398, (f) 423, (g) 448, and (h) 473 K. The C—H stretching and low-frequency regions are shown in A and B, respectively.

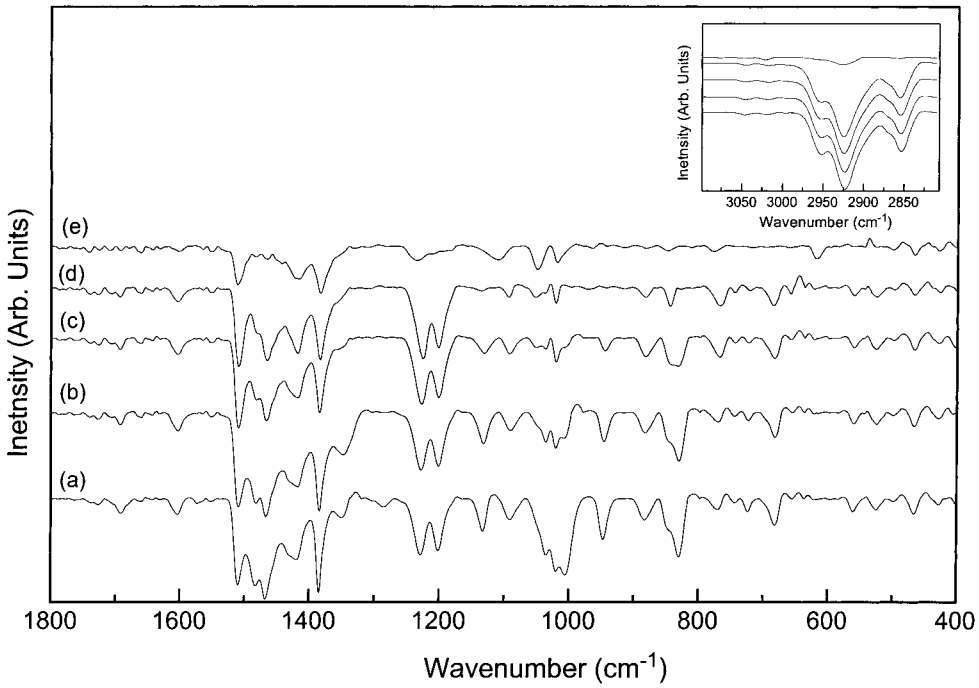

FIG. 4. The variable-temperature FT-IR spectra of BDMT-capped Ag clusters. The temperatures are (a) 298, (b) 348, (c) 373, (d) 423, and (e) 448 K. The corresponding C—H regions are shown in the inset.

the methylene modes at 1198 and 1228 cm^{-1}) observed upon increase in temperature, only reduction in intensity due to the desorption of monolayers from the cluster surface is observed. This is particularly noticeable beyond 423 K; the spectrum at 448 K shows the complete absence of the C—S stretching mode at 676 cm^{-1}. It is interesting to note the absence of shift in any of the bands, even at 448 K. The ring deformation band retains its shape even at 448 K, showing that the still-adsorbed fraction of the monolayer retains its structure. This observation is similar to that seen in the case of 2D SAMs, where the monolayers undergo no structural change on increase in temperature (16).

X-Ray Photoelectron Spectroscopy

Figure 5 shows the X-ray photoelectron spectra of BDMT-capped Au and Ag clusters. The spectra show gold $4f_{7/2}$ peak at 84 eV binding energy (BE) and silver $3d_{5/2}$ at 368 eV, characteristic of bulk Au^0 and Ag^0 (3a), respectively. Absence of any observable shift indicates that the fraction of atoms involved in bonding is low in the clusters. Even for a cluster of 2.8-nm core diameter, only 10% of the total number of atoms are bound to thiolate groups (4), and the absence of Au^I in XPS is not unexpected. Final state effects do not seem to shift the peak position greatly in this size range as seen earlier (4).

In one of our recent investigations of metal cluster liquids by X-ray photoelectron spectroscopy, we found the presence of Ag(I) on the surface of the clusters (20). This investigation was possible on a smooth film of the sample, which was prepared by melting the monolayer-capped metal superlattice solid (21), leading to a free flowing liquid. Upon cooling, the surface formed is smooth enough to show angle-dependent variation of intensity in the X-ray photoelectron spectrum. In the case of powder samples of BDMT capped clusters, due to difficulty in making smooth surfaces, such a measurement was not undertaken.

The sulfur 2*p* regions for gold and silver clusters are shown in Fig. 6. The broad nature of sulfur peaks indicates the presence of more than one kind of sulfur. The thiolate peak in the clusters, as well as planar monolayers, is observed in the range 162–164 eV BE (4). In both cases, the peak maximum is shifted from the characteristic thiolate position. We attribute the intensity in the high binding energy side of the spectrum to the X-ray beam induced damage of the monolayer. Although the nature of the surface sulfur group is unclear, it may be noted that even in relatively clean UHV conditions, this degradation is observed (22). Since the IR spectra of the clusters do not support the presence of thiols, coadsorption of thiols is not the cause of the increased width. X-ray induced disulfide formation could also contribute to the width, but it has not been confirmed independently.

Mass Spectrometry

Mass spectrometry gives valuable molecular information. Figure 7 shows the mass spectra obtained from silver and gold clusters capped with BDMT. Peaks at m/z 466, 353, 254, and 156 can be attributed to the phase transfer reagent. These are

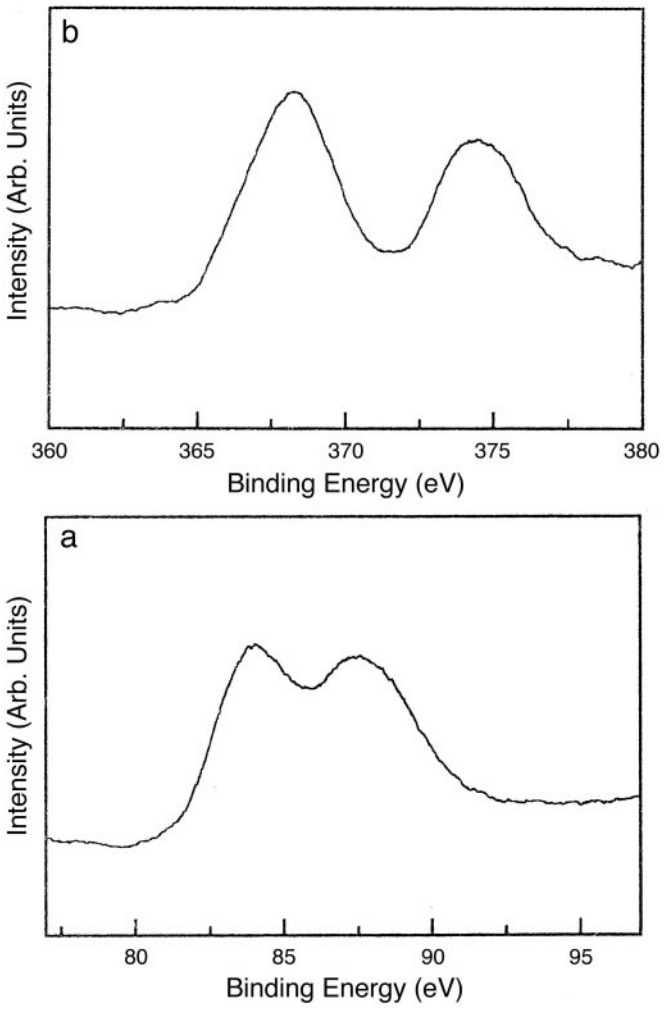

FIG. 5. The Al$K\alpha$ induced X-ray photoelectron spectra in the (a) Au 4*f* and (b) Ag 3*d* regions of the BDMT-capped gold and silver clusters, respectively.

due to the molecular ion of the phase transfer reagent $(C_8H_{17})_4N$ and its fragments. The first fragment appears at m/z 353 due to the loss of one *n*-octyl group. This subsequently loses a C_7H_{15} group to yield an intense peak at m/z 254, which undergoes two C_7H_{14} losses; only one is manifested in Fig. 7. In order to ascertain the origin of peaks, collision-induced dissociation (CID) mass spectra of some of the peaks were measured. The CID mass spectrum of m/z 254 shows two systematic 98 (C_7H_{14}) losses, yielding two peaks at m/z 156 and 58.

The mass peaks due to BDMT are also shown in the spectrum. These peaks are observed at m/z 338, 304, 168, 136, 104, and 91. The molecular ion is observed at m/z 168 ($C_8H_8S_2$). Its dimer is seen at m/z 336, and a loss of sulfur is seen as a peak at m/z 304. The peak at m/z 136 is due to a loss of sulfur from the molecular ion. The CH_2–C_6H_4–CH_2 moiety is seen at m/z 104. The tropylium ion (m/z 91) is one of the major fragments of the xylyl group. The mass spectrum is completely in agreement with the molecular species at the surface.

The spectrum does not show any specific enhancement of peaks on either of the surfaces. In either case, the peaks are due to the fragments of the dithiolate at the surface, no monothiolate fragment is seen.

DISCUSSION AND CONCLUSION

The most striking aspect of the results is the considerable difference in the adsorption geometries of the molecules on the 2D and 3D SAMs. Whereas the molecule adsorbs in the monothiolate form in the case of the Au 2D SAM, the adsorption is in the dithiolate form in the case of the 3D SAM. There is no such difference in the case of Ag; in both cases the adsorbate is in the dithiolate form. The difference in adsorbate geometry showed up as the difference in the temperature-dependent Raman spectra of the two in the case of the 2D SAMs. For cluster monolayers, the changes in the temperature-

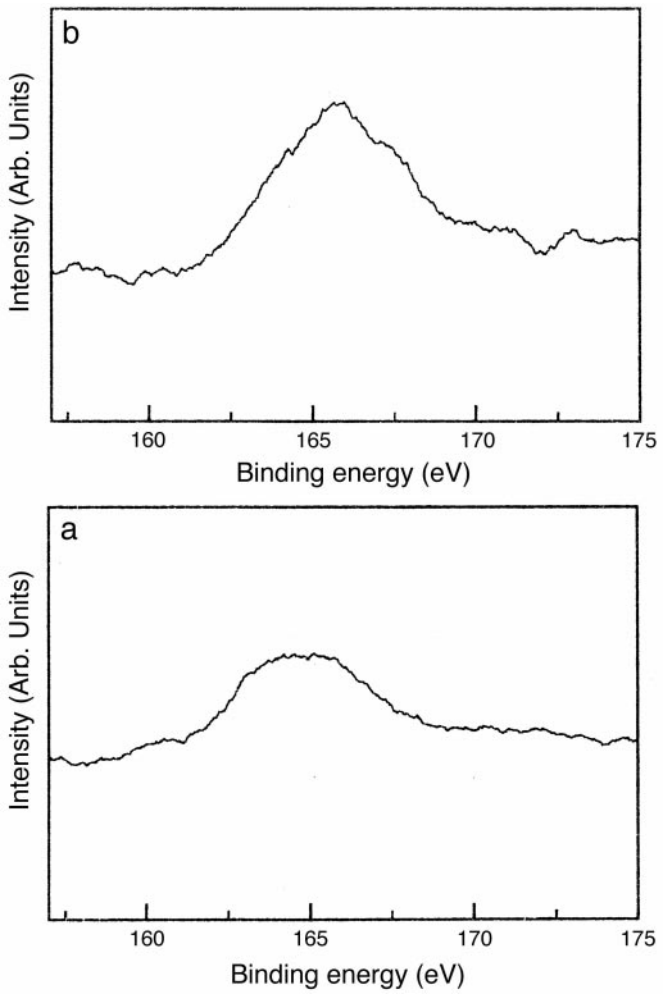

FIG. 6. The Al$K\alpha$ induced X-ray photoelectron spectra in the S2*p* region of BDMT-capped (a) Au and (b) Ag clusters.

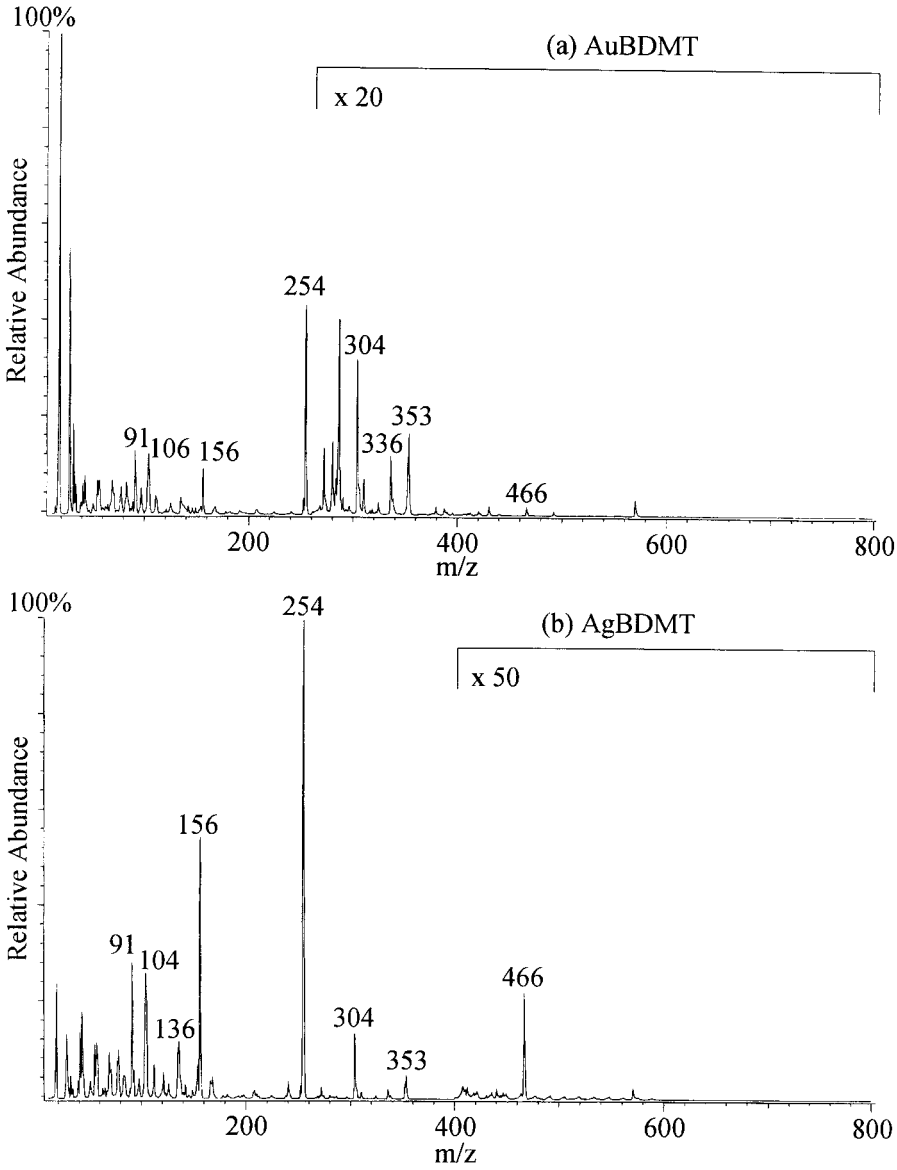

FIG. 7. Mass spectra of BDMT-capped (a) Au and (b) Ag clusters. Mass numbers of the peaks of importance are labeled.

dependent IR spectra are small and are limited to differences in the orientation of the adsorbates.

How can such a difference in the adsorption geometry occur between the 2D and 3D SAMs? We offer the following tentative explanation. In the case of the 2D SAMs the surface atomic structure is static within the time scale of initial adsorption and subsequent organization. Others and we have shown that the kinetics of these two events are markedly different (12a, 23). For the 3D SAM, the surface structure is evolving in the time scale of adsorption. Although the kinetics of self-organization is slow and will be substantially different from that of the cluster growth, this process is only of negligible importance here since the molecular dimension is small. Thus as the cluster surface is evolving, the molecule in its vicinity gets adsorbed to the available sites. For a surface site, it is possible that the thiol group of a molecule already bound to the surface with the other thiol group is closer to it than that of an unbound molecule. It is also important that the surface is not flat but has some definite curvature that makes this molecular maneuver more possible. This implies that there is some definite delay between adsorption at different sites. During such a delay, molecular reorientation is possible to minimize energy. In the case of the 2D SAM, all the available adsorption sites are occupied as soon as the exposure occurs, and forces of self-organization will decide which of the sites will be occupied ultimately.

ACKNOWLEDGMENTS

T.P. thanks the Department of Science and Technology, Government of India, for supporting his research programs on monolayers. The mass spectra were recorded in the laboratory of Prof. Graham Cooks of Purdue University, where T.P. was a senior Fulbright Fellow.

REFERENCES

1. See, for a recent review of the area, Hostetler, M. J., and Murray, R. W., *Current Opinion Colloid Interface Surf.* **2,** 42 (1997).
2. (a) Wang, Y., and Herron, N., *J. Phys. Chem.* **95,** 525 (1991). (b) Schmid, G., *Chem. Rev.* **92,** 1709 (1992). (c) Hoffman, A. J., Mills, G., Yee, H., and Hoffman, M. R., *J. Phys. Chem.* **96,** 5546 (1992). (d) Green, S. J., Stokes, J. J., Hosteller, M. J., Pietron, J., and Murray, R. W., *J. Phys. Chem.* **101,** 2663 (1997). (e) Storhoff, J. J., Elghanian, R., Mucic, C., Mirkin, C. A., and Letsinger, R. L., *J. Am. Chem. Soc.* **120,** 1959 (1998). (f) Mandler, D., and Turyan, I., *Electroanalysis* **8,** 207 (1996).
3. (a) Brust, M., Walker, M., Bethell, D., Schiffrin, D. J., and Whyman, R., *J. Chem. Soc. Chem. Commun.*, 801 (1994). (b) Vijaya Sarathy, K., Kulkarni, G. U., and Rao, C. N. R., *J. Chem. Soc. Chem. Commun.*, 537 (1997). (c) Vijaya Sarathy, K., Raina, G., Yadav, R. T., Kulkarni, G. U., and Rao, C. N. R., *J. Phys. Chem. B* **101,** 9876 (1997). (d) Heath, J. R., Knobler, C. M., and Leff, D. V., *J. Phys. Chem. B* **101,** 189 (1997). (e). Reetz, M. T., and Helbig, W., *J. Am. Chem. Soc.* **116,** 7401 (1994). (f) Duteil, A., Schmid, G., and Meyer-Zeika, W., *J. Chem. Soc. Chem. Commun.* 31 (1995). (g) Duff, D. G., Baiker, A., and Edwards, P. P., *J. Chem. Soc. Chem. Commun.*, 96 (1993). (h) Kataby, G., Prozorov, T., Koltypin, Y., Cohen, H., Sukenic, C. N., Ulman, A., and Gedanken, A. *Langmuir* **13,** 6151 (1997).
4. Hostetler, M. J., Wingate, J. E., Zhong, C. J., Harris, J. E., Vachet, R. W., Clark, M. R., Londono, J. D., Green, S. J., Stokes, J. J., Wignall, G. D., Glish, G. L., Porter, M. D., Evans, N. D., and Murray, R. W., *Langmuir* **14,** 17 (1998).
5. Shi, J., Gider, S., Babcock, K., and Awschalom, D. D., *Science*, **271,** 937 (1996).
6. (a) Ulman, A., *"An Introduction to Ultrathin Organic Films: From Langmuir Blodgett to Self Assembly."* Academic Press, New York, 1991. (b) Ulman, A., *Chem. Rev.* **96,** 1533 (1996).
7. (a) Terril, R. H., Postlethwaite, T. A., Chen, C.-H., Poon, C.-D., Terzis, A., Chen, A., Hutchison, J. E., Clark, M. R., Wignall, G., Londono, J. D., Superfine, R., Falvo, M., Johnson, C. S., Jr., Samulski, E. T., and Murray, R. W., *J. Am. Chem. Soc.* **117,** 12537 (1995). (b) Brust, M., Fink, J., Bethell, D., Schiffrin, D. J., and Kiely, C., *J. Chem. Soc. Chem. Commun.*, 1655 (1995). (c) Leff, D. V., Ohara, P. C., Heath, J. R., and Gelbart, W. M., *J. Phys. Chem.* **99,** 7036 (1995). (d) Leff, D. V., Brandt, L., and Heath, J. R., *Langmuir* **12,** 4723 (1996). (e) Hosteller, M. J., Stokes, J. J., and Murray, R. W., *Langmuir* **12,** 3604 (1996). (f) Johnson, S. R., Evans, S. D., Mahon, S. W., and Ulman, A., *Langmuir* **13,** 51 (1997). (g) Alvarez, M. M., Khoury, J. T., Schaaff, T. G., Shafigullin, M. N., Vezmar, I., and Whetten, R. L., *J. Phys. Chem. B* **101,** 3706 (1997). (h) Badia, A., Cuccia, L., Demers, L., Morin, F., and Lennox, R. B., *J. Am. Chem. Soc.* **119,** 2682 (1997).
8. Ingram, R. S., Hosteller, M. J., Murray, R. W., Schaaff, T. G., Khoury, J. T., Whetten, R. L., Bigioni, T. P., Guthrie, D. K., and First, P. N., *J. Am. Chem. Soc.* **119,** 9279 (1997).
9. Badia, A., Singh, S., Demers, L., Cuccia, L., Brown, G. R., and Lennox, R. B., *Chem. Eur. J.* **2,** 359 (1996).
10. Templeton, A. C., Hosteller, M. J., Kraft, C. T., and Murray, R. W., *J. Am. Chem. Soc.* **120,** 1906 (1998).
11. Ingram, R. S., Hosteller, M. J., and Murray, R. W. *J. Am. Chem. Soc.* **119,** 9175 (1997).
12 (a) See, for example, Bain, C. D., Troughton, E. B., Tao, Y. T., Evall, J., Whitesides, G. M., and Nuzzo, R. G., *J. Am. Chem. Soc.* **111,** 321 (1989). (b) Finkelea, H. O., Avery, S., and Lynch, M., *Langmuir* **3,** 409 (1987). (c) Bain, C. D., Davies, P. B., Ong, T. H., Ward, R. N., and Brown, M. A., *Langmuir* **7,** 1563 (1991). (d) Whitesides, G. M., and Laibinis, P. E., *Langmuir* **6,** 87 (1990). (e) Allara, D. L., and Nuzzo, R. G., *Langmuir* **1,** 52 (1985). (f) Chidsey, C. E. D., Liu, G. Y., Rountree, P., and Scoles, G., *J. Chem. Phys.* **91,** 4421.(1989). (g) Tao, Y.-T., Wu, C.-C., Eu, J.-Y., and Lin, W.-L., *Langmuir* **13,** 4018 (1997).
13. See, for example, (a) Porter, M. D., Bright, T. B., Allara, D. L., and Chidsey, C. E. D., *J. Am. Chem. Soc.* **109,** 3559 (1987). (b) Nuzzo, R. G., Dubois, L. H., and Allara, D. L., *J. Am. Chem. Soc.* **112,** 558 (1990). (c) Nuzzo, R. G., Fusco, F. A., and Allara, D. L., *J. Am. Chem. Soc.* **109,** 2358 (1987).
14. (a) Kang, S. Y., and Kim, K., *Langmuir* **14,** 226 (1998). (b) Harfenist, S. A., Wang, Z. L., Alvarez, M. M., Vezmar, I., and Whetten, R. L., *J. Phys. Chem.* **100,** 13904 (1996).
15. Patil, V., Mayya, K. S., Pradhan, S. D., and Sastry, M., *J. Am. Chem. Soc.* **119,** 9281 (1997).
16. Murty, K. V. G. K., Venkataramanan, M., and Pradeep, T., *Langmuir* **14,** 5446 (1998).
17. West, A. R., *"Solid State Chemistry and Its Applications."* Wiley, New York, 1987.
18. (a) Johnson, E., and Aroca, R., *J. Phys. Chem.* **99,** 9325 (1995). (b) Moskovits, M., *J. Chem. Phys.* **77,** 4408 (1982).
19. Lee, T. G., Kim, K., and Kim, M. S., *J. Phys. Chem.* **95,** 9950 (1991).
20. Sandhyarani, N., Resmi, M. R., Unnikrishnan, R., Vidyasagar, K., Shuguang Ma, Antony, M. P., Panneer Selvam, G., Visalakshi, V., Chandrakumar, N., and Pradeep, T., *J. Am. Chem. Soc.*, in press.
21. Sandhyarani, N., Pradeep, T., and Vidyasagar, K., *Chem. Mater.*, in press.
22. Colvin, V. L., Goldstein, A. N., and Alivisatos, A. P., *J. Am. Chem. Soc.* **114,** 5221 (1992).
23. Sandhyarani, N., and Pradeep, T., *Vacuum* **49,** 279 (1998).